Science Signaling
AAAS

www.sciencesignaling.org/cgi/content/full/5/229/ra44/DC1

Supplementary Materials for

Direct Modification and Activation of a Nuclear Receptor–PIP_2 Complex by the Inositol Lipid Kinase IPMK

Raymond D. Blind, Miyuki Suzawa, Holly A. Ingraham*

*To whom correspondence should be addressed. E-mail: holly.ingraham@ucsf.edu

Published 19 June 2012, *Sci. Signal.* **5**, ra44 (2012)
DOI: 10.1126/scisignal.2003111

The PDF file includes:

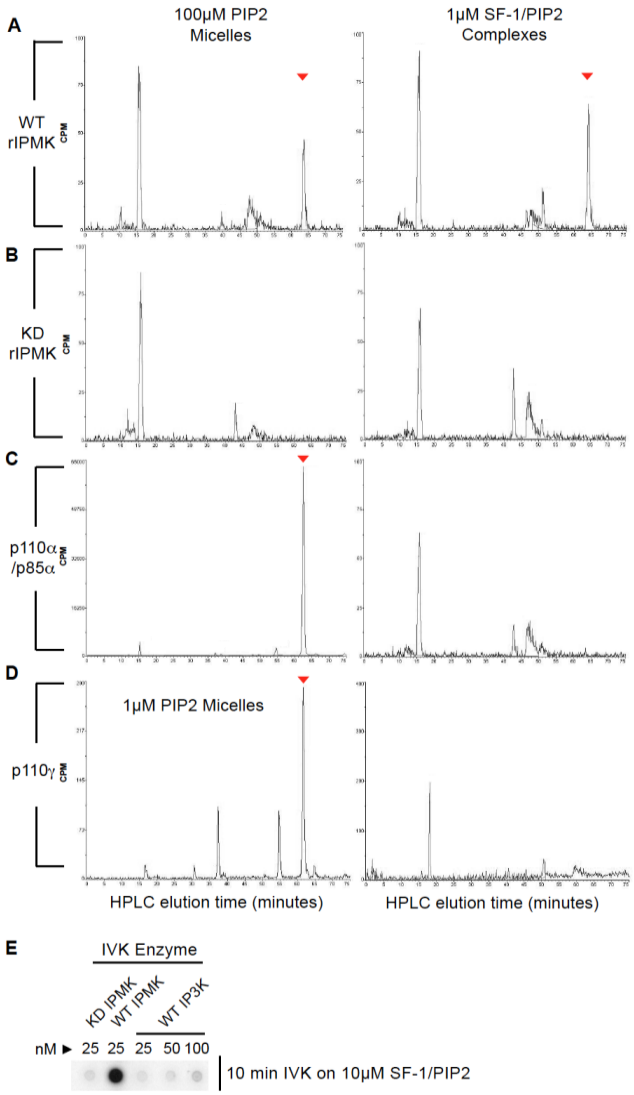

Fig. S1. p110γ, the kinase dead rIPMK mutant (D127A), and IP3K fail to generate PIP_3 from SF-1–PIP_2. HPLC chromatographs of glyceroinositol head groups after ^{32}P-γATP in vitro kinase reactions using 100 nM (**A**) wild-type (WT) rIPMK, (**B**) kinase dead (KD) rIPMK, (**C**) human p110α–p85α, or (**D**) p110γ, incubated with either PIP_2–phosphatidylserine micelles (left panels) or 1 μM SF-1–PIP_2 substrate (right panels), as indicated, for 30 min at 37°C. Migration of glyceroinositol (1,3,4,5)P following deacylation of PIP_3 is indicated with red arrowheads. (**E**) Autoradiography of 10 min in vitro kinase reactions on 10 μM SF-1–PIP_2 analyzed by nitrocellulose capture, using the indicated concentrations of indicated enzymes. Representative data from at least two independent experiments are shown.

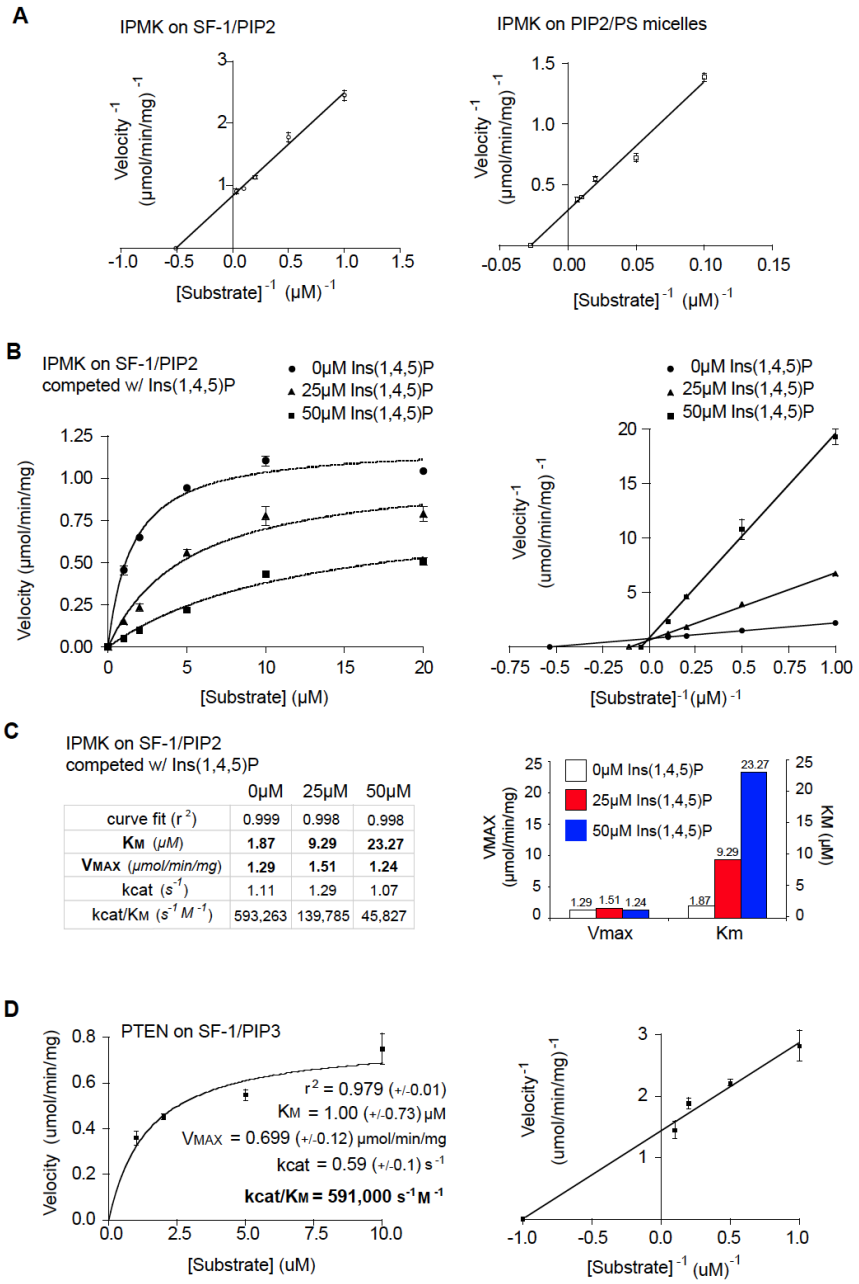

	0µM	25µM	50µM
curve fit (r^2)	0.999	0.998	0.998
KM (*µM*)	**1.87**	**9.29**	**23.27**
VMAX (*µmol/min/mg*)	**1.29**	**1.51**	**1.24**
kcat (s^{-1})	1.11	1.29	1.07
kcat/KM ($s^{-1} M^{-1}$)	593,263	139,785	45,827

Fig. S2. Enzyme/substrate kinetic parameters and competitive inhibition by Ins(1,4,5)P of IPMK activity on SF-1–PIP_2. Human IPMK velocities plotted against increasing substrate concentrations as measured by nitrocellulose capture assays of in vitro kinase reactions. Data were fit to (**A**) linear double-reciprocal (Lineweaver-Burke) and non-linear (Michaelis-Menton; refer to Fig. 2) curves by GraphPad Prism software. (**B**) Non-linear and linear curve fits of IPMK reaction velocities on SF-1–PIP_2 as determined above, except in the presence of the indicated concentrations of Ins(1,4,5)P. Data are presented fitted to non-linear and linear plots, fitted as in (A). (**C**) Table of kinetic parameters at each

Ins(1,4,5)P concentration shows a constant V_{MAX}, with a changing K_M; values are presented in the bar graph (right). **(D)** PTEN activity on SF-1−PIP_2 was measured by extracting the PTEN reaction product (SF-1−PIP_2) into 1:1 MeOH:$CHCl_3$ and coupling to a p110α−p85α ^{32}P-γATP in vitro kinase reaction. Data were fit to non-linear Michaelis-Menton and linear double-reciprocal Lineweaver-Burke curves by GraphPad Prism software. Data represent at least three independent experiments.

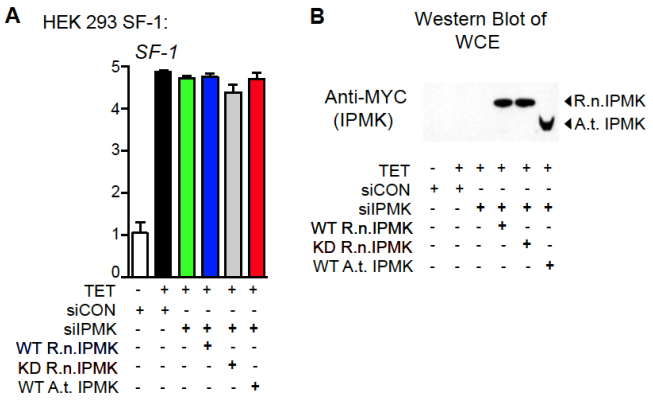

Fig. S3 Overexpression of different IPMKs does not affect *SF-1* transcript abundance. (**A**) *SF-1* transcript abundance after transfection of control (siCON) or IPMK (siIPMK) siRNAs followed by transient transfection of indicated IPMK expression constructs. (**B**) Expression of myc-tagged IPMK proteins in HEK 293 SF-1 cells treated identically as in (A). For Panel A, data represent three independent experiments; for Panel B, representative data from two independent experiments are shown.

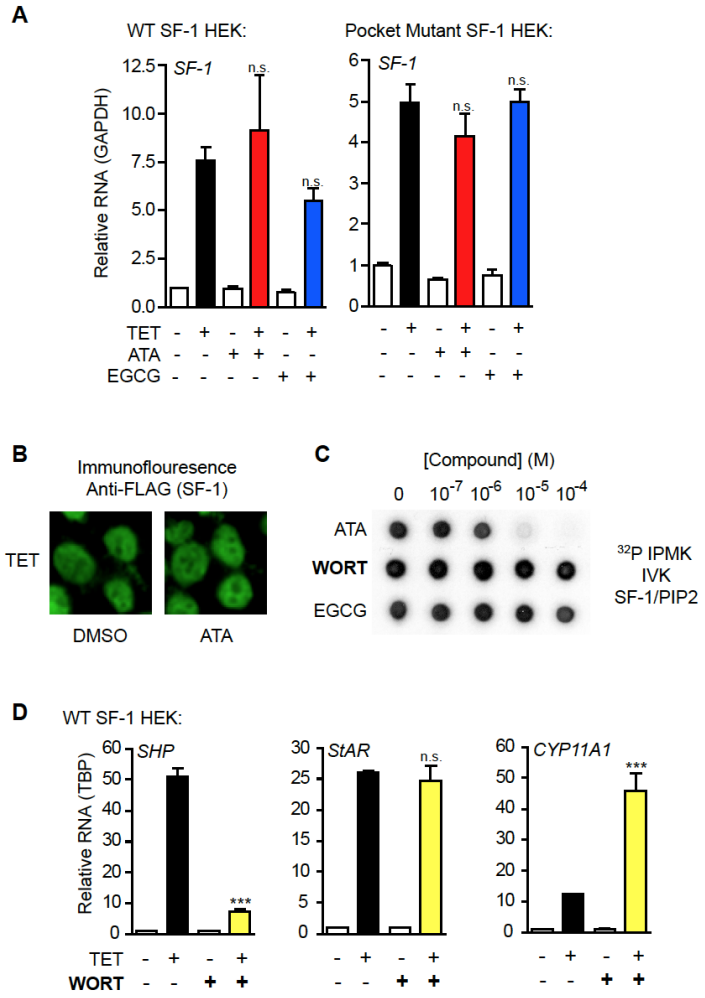

Fig. S4. *SF-1* transcript abundance and SF-1 nuclear localization are unaffected by ATA and EGCG, and wortmannin does not recapitulate ATA effects on SF-1 target gene expression. (**A**) *SF-1* transcript abundance was determined in HEK 293 cells expressing wild-type or pocket mutant (A270W, L345F) SF-1 following ATA or EGCG treatment. (**B**) Immunocytochemistry of 3X-FLAG tagged SF-1 in HEK 293 SF-1 cells treated with vehicle or ATA. (**C**) IPMK activity on SF-1–PIP_2 in the presence of indicated compounds at indicated concentrations. (**D**) qPCR measuring transcript abundance of the indicated genes in HEK 293 SF-1 cells after 14 hours treatment with wortmannin (WORT, 10 μM) or DMSO vehicle control. Representative data from at least three independent experiments are shown.

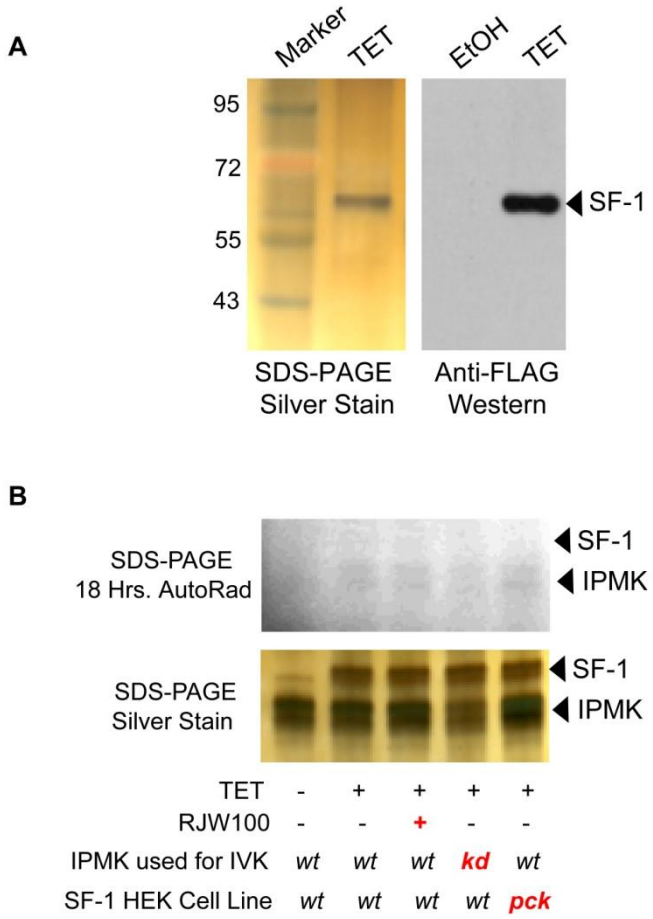

Fig S5. SF-1 purified from HEK 293 cells is not phosphorylated by IPMK. (**A**) Silver stained SDS-PAGE of FLAG-peptide eluates from TET-induced HEK 293 SF-1 cells demonstrating purity of SF-1 protein. Molecular weight standards are indicated to the left. Western blot of FLAG peptide eluates from EtOH and TET-induced HEK 293 SF-1 cells probed with anti-FLAG antibodies. (**B**) Autoradiography of in vitro kinase reactions (shown in Fig. 6A) separated by SDS-PAGE (upper panel). Following exposure for 18 hours, gels were silver stained to confirm equal loading of lanes and the presence of all SF-1 and IPMK proteins; experimental conditions in each reaction are indicated. Representative data from at least three independent experiments are shown.

Table S1. RT-qPCR Primers

Gene	Accession	Forward Primer Sequence	Reverse Primer Sequence
mSF-1 (NR5A1)	NM_139051	CGTCTGTCTCAAGTTCCTCATCCT	TCCTTTACGAGGCTGTGGTTGT
hSHP (NR0B2)	NM_021969	GCTTAGCCCCAAGGAATATGC	TTGGAGGCCTGGCACATC
hStAR	NM_000349	CCCATGGAGAGGCTCTATGAA	GTTCCACTCCCCCATTGCT
hCYP17A1	NM_000102	AGGACTTCTCTGGGCGGCCT	GTGTGCGCCAGAGTCAGCGA
hCYP11A1	NM_000781	GGGTCGCCTATCACCAGTATT	GCTGCCGACTTCTTCAACAG
hGAPDH	NM_002046	CAAGGTCATCCATGACAACTTTG	GGCCATCCACAGTCTTCTGG
hTBP	NM_003194	CCTAAAGACCATTGCACTTCGT	AGCAAACCGCTTGGGATTA

Table S2. ChIP-qPCR Primers

Gene	Accession	Forward primer sequence	Reverse primer sequence
hHSP70	NM_198431	TCTGGAGAGTTCTGAGCAGG	CCCTTCTGAGCCAATCACCG
hStAR	NM_000349	CCACAAACGGCCAAGCA	CGCCATCACTCACTGTGCAA